Butadiene Complexes of Titanium(II) and Titanium(0): Synthesis, Butadiene Dimerization Catalysis, and Crystal Structures of $TiMe_2(\eta^4\text{-}1,4\text{-}C_4H_4Ph_2)(dmpe)$ and $Ti(\eta^4\text{-}C_4H_6)_2(dmpe)$

Michael D. Spencer, Scott R. Wilson, and Gregory S. Girolami*

School of Chemical Sciences, University of Illinois at Urbana-Champaign, 601 South Goodwin Avenue, Urbana, Illinois 61801

Received August 5, 1996[⊗]

The titanium(II) alkyl *trans*-$TiMe_2(dmpe)_2$, where dmpe is 1,2-bis(dimethylphosphino)-ethane, reacts with 1,3-butadiene and *trans,trans*-1,4-diphenyl-1,3-butadiene at −20 °C to produce the titanium(II) butadiene complexes $TiMe_2(\eta^4\text{-}C_4H_4R_2)(dmpe)$, where R is H or Ph. NMR spectra are consistent with structures in which the methyl groups are mutually *cis*, and this has been verified crystallographically for the 1,4-diphenylbutadiene complex. These molecules are fluxional on the NMR time scale, and the activation parameters for exchange are $\Delta H^{\ddagger} = 9.1 \pm 0.2$ kcal mol^{-1} and $\Delta S^{\ddagger} = 3 \pm 1$ eu for the 1,4-diphenylbutadiene complex. The process that exchanges the two Ti−Me groups, the two ends of the dmpe ligand, and the two ends of the butadiene ligand is proposed to be a trigonal twist, although we cannot entirely rule out the possibility that the exchange involves five-coordinate intermediates generated by dissociation of one "arm" of a chelating ligand. If the reaction of $TiMe_2(dmpe)_2$ and 1,3-butadiene is allowed to proceed at −20 °C for prolonged periods (>12 h), a second titanium "butadiene" complex is formed, which has been identified as the titanium(IV) η^3,η^1-octa-1,6-diene-1,8-diyl complex $TiMe_2(\eta^3,\eta^1\text{-}C_8H_{12})(dmpe)$. Warming a solution of $TiMe_2(dmpe)_2$ and 1,3-butadiene to 25 °C results in the catalytic dimerization of butadiene to the Diels−Alder dimer 4-vinylcyclohexene at rates of 5 turnovers/h. A mechanism for the catalytic dimerization is proposed, which involves coupling of two butadiene ligands to form a divinyltitanacyclopentane species, allylic rearrangement to a vinyltitanacycloheptene intermediate, and reductive elimination to form the cyclic product. Treatment of $TiMe_2(dmpe)_2$ with 1,3-butadiene in the presence of $AlEt_3$ results in reduction to the titanium(0) complex $Ti(\eta^4\text{-}C_4H_6)_2(dmpe)$, which has also been crystallographically characterized. Unlike the behavior seen for certain other early transition metal butadiene complexes, in both $Ti(\eta^4\text{-}C_4H_6)_2(dmpe)$ and $TiMe_2(\eta^4\text{-}C_4H_4Ph_2)(dmpe)$ the butadiene ligands are bound like true dienes. We propose that the preferred bonding mode for butadiene complexes of the lower valent early transition metals is the π,η^4 mode and that increasing σ^2,π character is introduced only when there are significant steric repulsions between the ancillary ligands and the *meso* butadiene substituents.

Introduction

Butadiene and its oligomers are useful feedstocks in the industrial production of organic chemicals. For example, dimers of butadiene, such as 1,5-cyclooctadiene, 1,3,7-octatriene, and 4-vinylcyclohexene, are used as precursors for flame retardants, terpenoid and sesquiterpenoid compounds of biological interest, and fragrances.[1−3] Other industrial applications include the synthesis of linear α,ω-dienes from 1,5-cyclooctadiene in Shell's FEAST process and the synthesis of styrene by dehydrogenation of 4-vinylcyclohexene. If the dimerization of butadiene or its substituted analogues is conducted under H_2, terminal octenes can be produced that can be used in the manufacture of linear low-density polyethylene.[1−3]

Although nickel and palladium compounds are most commonly used to catalyze the dimerization of butadiene,[4−6] some early transition metal complexes can also promote these reactions. Interestingly, while the group 10 complexes generally give cyclic dimers, homogeneous early transition metal catalysts give linear dimers. For example, $Cp_2Zr(\eta^4\text{-diene})$ and $Cp_2Hf(\eta^4\text{-diene})$ complexes

[⊗] Abstract published in *Advance ACS Abstracts,* June 1, 1997.

(1) Parshall, G. W. *Homogeneous Catalysis*; Wiley: New York, 1980; pp 65−70. Masters, C. *Homogeneous Transition-Metal Catalysis—A Gentle Art*; Chapman and Hall: London, 1981; pp 144−153.

(2) Kaminsky, W.; Kramolowsky, R. *Inorganic Reactions and Methods*; Zuckermann, J. J., Norman, A. D., Eds.; VCH Publishers: New York, 1993; pp 276−298.

(3) Sun, H. N.; Wristers, J. P. *Kirk-Othmer Encyclopedia of Chemical Technology*, 4th ed.; Kruschwitz, J. I., Howe-Grant, M., Eds.; Wiley: New York, 1992; Vol. 4, pp 663−690.

(4) (a) Keim, W.; Behr, A.; Röper, M. *Comprehensive Organometallic Chemistry*; Wilkinson, G., Stone, F. G. A., Abel, E. W., Eds.; Pergamon: New York, 1982; Vol. 8, pp 371−462; (b) Jolly, P. W. *Comprehensive Organometallic Chemistry*; Wilkinson, G., Stone, F. G. A., Abel, E. W., Eds.; Pergamon: New York, 1982; Vol. 8, pp 671−711.

(5) Tsuji, J. *Adv. Organomet. Chem.* **1979**, *17*, 141−193

(6) For the use of asymmetric nickel catalysts to convert butadiene to optically-active 4-vinylcyclohexene, see: Richter, W. J. *J. Mol. Catal.* **1981**, *13*, 201−206. Cros, P.; Buono, G.; Peiffer, G.; Denis, D.; Mortreux, A.; Petit, F. *New J. Chem.* **1987**, *11*, 573−579. For Diels−Alder dimerizations of butadiene to 4-vinylcyclohexene catalyzed by metals outside of groups 4 or 10, see: *Chem. Eng. News* **1994**, *72*(25), 31−32. Mortreux, A.; Bavay, J. C.; Petit, F. *Nouv. J. Chem.* **1980**, *4*, 671−676. tom Dieck, H.; Dietrich, J. *Angew. Chem., Int. Ed. Engl.* **1985**, *24*, 781−783. Bonnesen, P. B.; Puckett, C. L.; Honeychuck, R. V.; Hersh, W. H. *J. Am. Chem. Soc.* **1989**, *111*, 6070−6081.

S0276-7333(96)00655-3 CCC: $14.00

dimerize isoprene to substituted C_8 trienes.[7] The dimerization of butadiene to linear C_8 alkenes can also be achieved by using low-valent titanium catalysts generated *in situ* by treatment of $CpTiCl_3$, $CpTiCl_2$, or Cp_2TiCl_2 with "Mg(isoprene)" or Grignard reagents.[8] The zero-valent butadiene complexes $Ti(\eta^4\text{-}C_4H_6)_2(dmpe)$ and $Zr(\eta^4\text{-}C_4H_6)_2(dmpe)$ also catalyze the dimerization of butadiene to a complex mixture of C_8 alkenes, but the nature of the alkenes was not identified.[9,10] Butadiene polymers are also produced in these reactions. The allyl complex $Zr(\eta^8\text{-}C_8H_8)(\eta^3\text{-}C_3H_5)_2$ catalyzes the dimerization of butadiene to 1,3,6-octatriene.[11]

We have reported that the Ti^{II} complex *trans*-$TiMe_2(dmpe)_2$, where dmpe is 1,2-bis(dimethylphosphino)ethane), is a catalyst for the dimerization of ethylene to 1-butene.[12] We now describe the reactions of $TiMe_2(dmpe)_2$ with 1,3-butadiene and *trans,trans*-1,4-diphenyl-1,3-butadiene. The formation of butadiene coordination complexes and the catalytic dimerization of butadiene is described. Interestingly, $TiMe_2(dmpe)_2$ is the first homogeneous early transition metal catalyst that dimerizes butadiene to a *cyclic* product, 4-vinylcyclohexene. Mechanistic aspects of the dynamic processes and catalytic chemistry that these butadiene complexes undergo, and a unified explanation of the widely-varying structures of group 4 butadiene complexes, are also discussed.

Results and Discussion

Reaction Chemistry of $TiMe_2(dmpe)_2$ toward Butadiene. Several different organometallic products have been obtained by addition of butadiene to the titanium(II) alkyl[13] $TiMe_2(dmpe)_2$; the complex isolated depends on the temperature and reaction time. When $TiMe_2(dmpe)_2$ is treated with 20 equiv of 1,3-butadiene at −72 °C and then warmed to −20 °C, a green-blue solution is generated from which the new titanium(II) butadiene complex $TiMe_2(\eta^4\text{-}C_4H_6)(dmpe)$, **1**, can be isolated as a green oil. Complex **1** is thermally unstable

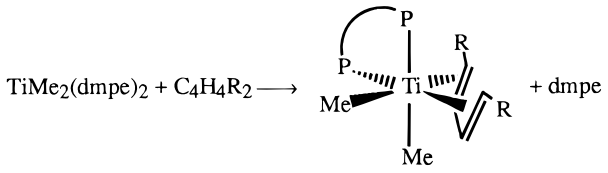

1, R = H

2, R = Ph

in solution and decomposes above 0 °C in the absence of excess butadiene.

A similar reaction of $TiMe_2(dmpe)_2$ with *trans,trans*-1,4-diphenyl-1,3-butadiene also results in the displacement of one dmpe ligand and the generation of $TiMe_2(\eta^4\text{-}1,4\text{-}C_4H_4Ph_2)(dmpe)$, **2**, which can be isolated as dichroic (red/green) crystals. We will show below that the methyl groups in the $TiMe_2(\eta^4\text{-}C_4H_4R_2)(dmpe)$ complexes are mutually *cis*; this arrangement is somewhat unexpected since the methyl groups in the starting material $TiMe_2(dmpe)_2$ are mutually *trans*.

Treatment of a toluene solution of *trans*-$TiMe_2(dmpe)_2$ with excess butadiene at −20 °C for prolonged periods (>12 h) produces a second titanium "butadiene" species which can be isolated by slowly removing the solvent at −72 °C. The resulting orange solid is moisture and oxygen sensitive.

As judged from its NMR spectra (see below), complex **3** has the stoichiometry $TiMe_2(C_8H_{12})(dmpe)$ in which the C_8H_{12} group consists of two butadiene molecules that have coupled to form an η^3,η^1-octa-1,6-diene-1,8-diyl ligand. At temperatures above −20 °C and in the

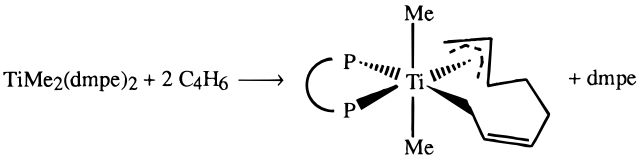

3

presence of excess butadiene, the "bis(butadiene)" complex **3** converts to the mono(butadiene) adduct **1**. This transformation occurs via reductive elimination of 4-vinylcyclohexene. In fact, the titanium(II) complex $TiMe_2(dmpe)_2$ serves as a catalyst for the dimerization of butadiene to 4-vinylcyclohexene (see below).

Treatment of $TiMe_2(dmpe)_2$ with 1,3-butadiene in the presence of triethylaluminum results in the rapid reduction of the titanium center and isolation of the titanium(0) bis(butadiene) complex $Ti(\eta^4\text{-}C_4H_6)_2(dmpe)_2$, **4**. Sealed NMR tube experiments show that this reaction occurs nearly quantitatively.

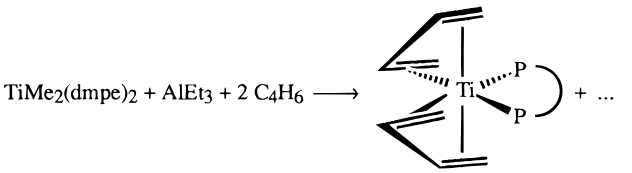

4

This blue diamagnetic complex has previously been prepared by reduction of $TiCl_4(dmpe)$ with sodium amalgam in the presence of butadiene[9] or by treatment of $TiCl_4(dmpe)$ with the magnesium butadiene reagent $Mg(C_4H_6)\cdot 2THF$.[14] Only one other titanium(0) butadiene complex is known, $Ti[\eta^4\text{-}1,4\text{-}C_4H_4(t\text{-}Bu)_2]_2$.[15]

Before turning to the solution dynamics of these complexes and a discussion of the catalytic butadiene dimerization chemistry, we will describe the solid state structures of the 1,4-diphenylbutadiene complex **2** and the bis(butadiene) complex **4**.

X-ray Crystal Structure of $TiMe_2(\eta^4\text{-}1,4\text{-}C_4H_4Ph_2)(dmpe)$. Crystals of **2** were grown from diethyl ether. Molecules of **2** lie on general positions within the unit cell, and one molecule resides in the asymmetric unit.

(7) Yasuda, H.; Nakamura, A. *Angew. Chem., Int. Ed. Engl.* **1987**, *26*, 723−742.
(8) Yamamoto, H.; Yasuda, H.; Tatsami, K.; Lee, K.; Nakamura, A.; Chen, J.; Kai, Y.; Kasai, N. *Organometallics* **1989**, *8*, 105−119.
(9) Beatty, R. P.; Datta, S.; Wreford, S. S. *Inorg. Chem.* **1979**, *18*, 3139−3145.
(10) Datta, S.; Wreford, S. S.; Beatty, R. P.; McNeese, T. J. *J. Am. Chem. Soc.* **1979**, *101*, 1053−1054.
(11) Kablitz, H.-J.; Wilke, G. *J. Organomet. Chem.* **1973**, *51*, 241−271.
(12) Spencer, M. D.; Morse, P. M.; Wilson, S. R.; Girolami, G. S. *J. Am. Chem. Soc.* **1993**, *115*, 2057−2059.
(13) Jensen, J. A.; Wilson, S. R.; Schultz, A. J.; Girolami, G. S. *J. Am. Chem. Soc.* **1987**, *109*, 8094−8096.
(14) Wreford, S. S.; Whitney, J. F. *Inorg. Chem.* **1981**, *20*, 3918−3924.
(15) Cloke, F. G. N.; McCamley, A. *J. Chem. Soc., Chem. Commun.* **1991**, 1470−1471.

Table 1. Crystal Data for $TiMe_2(\eta^4\text{-}1,4\text{-}C_4H_4Ph_2)$(dmpe), 2, and $Ti(\eta^4\text{-}C_4H_6)_2$(dmpe), 4

	2	**4**
T, °C	−75	−75
space group	$P2_1/n$	$P\bar{1}$
a, Å	8.884(2)	9.208(2)
b, Å	15.424(3)	13.245(5)
c, Å	17.199(4)	14.704(4)
α, deg	90	109.90(3)
β, deg	93.61(2)	96.32(2)
γ, deg	90	102.29(2)
V, Å^3	2352(3)	1615(2)
Z	4	4
d_{calcd}, g cm^{-3}	1.227	1.259
μ_{calcd}, cm^{-1}	5.00	7.00
size, mm	0.1 × 0.2 × 0.4	0.2 × 0.2 × 0.2
diffractometer	Enraf−Nonius CAD4	
radiation	Mo Kα, λ = 0.710 73 Å	
monochromator	graphite crystal, 2θ = 12°	
scan range, type	$2.0 \le 2\theta \le 48°$, ω/θ	
scan speed, width	2−16° min^{-1}, $\Delta\omega = 1.50\ (1.00 + 0.35 \tan\theta)°$	
no. of reflns, total	4247	5315
no. of reflns, unique	3691	4202
no. of reflns, $I > 2.58\sigma(I)$	1991	2277
R_i	0.020	0.032
R_F	0.047	0.046
R_{wF}	0.039	0.046
no. of variables	353	382
p factor	0.010	0.020

Table 2. Selected Bond Distances (Å) and Angles (deg) for $TiMe_2(\eta^4\text{-}1,4\text{-}C_4H_4Ph_2)$(dmpe), 2

Distances			
Ti−P(1)	2.598(2)	C(23)−H(23a)	0.97(5)
Ti−P(2)	2.629(2)	C(23)−H(23b)	0.92(5)
Ti−C(1)	2.452(6)	C(23)−H(23c)	0.94(5)
Ti−C(2)	2.311(6)	C(24)−H(24a)	1.02(5)
Ti−C(3)	2.283(6)	C(24)−H(24b)	0.86(6)
Ti−C(4)	2.427(6)	C(24)−H(24c)	0.92(5)
Ti−C(23)	2.169(7)	C(1)−H(1)	0.96(5)
Ti−C(24)	2.129(7)	C(2)−H(2)	0.87(5)
C(1)−C(2)	1.410(8)	C(3)−H(3)	0.98(5)
C(2)−C(3)	1.394(8)	C(4)−H(4)	0.98(5)
C(3)−C(4)	1.413(8)		

Angles			
P(1)−Ti−P(2)	72.94(5)	C(1)−Ti−C(2)	34.3(2)
P(1)−Ti−C(1)	88.2(1)	C(1)−Ti−C(3)	62.8(2)
P(1)−Ti−C(2)	114.4(2)	C(1)−Ti−C(4)	73.7(2)
P(1)−Ti−C(3)	149.5(2)	C(1)−Ti−C(23)	101.1(2)
P(1)−Ti−C(4)	148.5(1)	C(1)−Ti−C(24)	164.1(2)
P(1)−Ti−C(23)	78.7(2)	C(2)−Ti−C(3)	35.3(2)
P(1)−Ti−C(24)	103.5(2)	C(2)−Ti−C(4)	62.4(2)
P(2)−Ti−C(1)	87.8(1)	C(2)−Ti−C(23)	84.8(2)
P(2)−Ti−C(2)	115.7(1)	C(2)−Ti−C(24)	140.4(2)
P(2)−Ti−C(3)	112.4(2)	C(3)−Ti−C(4)	34.7(2)
P(2)−Ti−C(4)	80.7(1)	C(3)−Ti−C(23)	97.0(2)
P(2)−Ti−C(23)	149.9(2)	C(3)−Ti−C(24)	106.9(2)
P(2)−Ti−C(24)	85.4(2)	C(4)−Ti−C(23)	129.3(2)
C(23)−Ti−C(24)	91.9(3)	C(4)−Ti−C(24)	91.1(2)

Displacements (Å) out of the C(1)−C(2)−C(3)−C(4) Mean Plane			
Ti	1.944(1)	H(1)	−0.36(5)
C(5)	0.077(5)	H(2)	0.11(5)
C(11)	0.051(5)	H(3)	0.10(5)
		H(4)	−0.46(5)

Crystal data are collected in Table 1, and selected bond distances and angles are presented in Table 2.

The ligands in $TiMe_2(\eta^4\text{-}1,4\text{-}C_4H_4Ph_2)$(dmpe) are disposed in a distorted octahedral fashion about the titanium center (Figure 1). Unlike the starting material $TiMe_2(dmpe)_2$, which adopts a *trans* geometry, the Ti−Me groups in **2** are *cis* to each other and form a C−Ti−C angle of 91.9(3)°. The Ti−Me bond distances differ only slightly: the Ti−Me bond *trans* to the dmpe ligand of 2.169(7) Å is somewhat longer than the Ti−Me bond *trans* to the 1,4-diphenylbutadiene ligand of 2.129(7) Å. For comparison, the Ti−Me bond lengths in $TiMe_2(dmpe)_2$ are 2.217(2) Å. The shorter Ti−Me bond lengths in **2** may be a consequence of the π-accepting nature of the 1,4-diphenylbutadiene ligand, which should promote stronger σ-donation from the Ti−Me groups. Alternatively, the shorter Ti−Me distances in **2** may reflect the differing nature of the *trans* groups in the two compounds: strongly *trans*-labilizing methyl groups in $TiMe_2(dmpe)_2$ vs phosphine or alkene ligands in **2**.

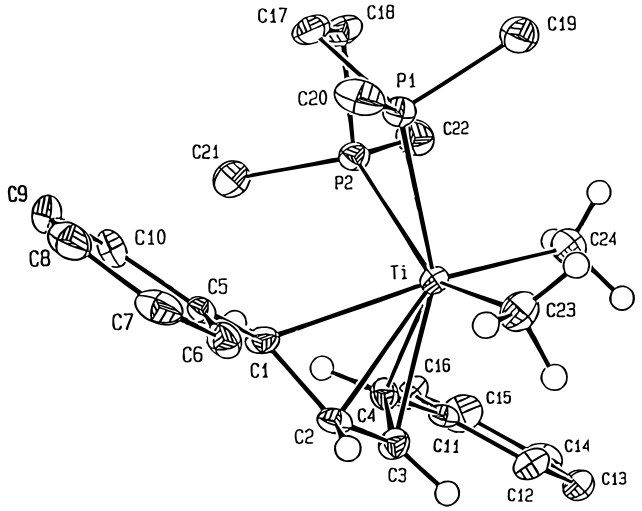

Figure 1. ORTEP diagram from the X-ray crystal structure of $TiMe_2(\eta^4\text{-}1,4\text{-}C_4H_4Ph_2)$(dmpe), **2**. The 35% probability ellipsoids are shown.

The titanium−phosphorus bond distances show differences that also may be ascribed to a *trans* influence. The Ti−P bond *trans* to the titanium methyl (2.629(2) Å) is slightly longer than the Ti−P bond *trans* to the diene ligand (2.598(2) Å). The titanium−phosphorus distances are longer than those of 2.520(1) Å in the parent compound $TiMe_2(dmpe)_2$ but lie within the range previously noted for other titanium phosphine complexes.[16]

The 1,4-diphenylbutadiene ligand is bound in an η^4-fashion and possesses an essentially planar carbon skeleton. The "open" edge of the ligand is oriented toward the Ti−P(2) bond (Figure 1). The titanium center lies 1.944 Å from the butadiene mean plane. The C−C distance between the interior carbon atoms of the butadiene framework is 0.018 Å shorter than the average C−C distance between the inner and outer carbon atoms; this pattern is consistent with the structures of $Fe(\eta^4\text{-diene})(CO)_3$ complexes[17,18] and $Hf(\eta^4\text{-}C_4H_6)_2$(dmpe),[14] in which the interior C−C distance is the shorter by ca. 0.02 and 0.054(7) Å, respectively. A comparison of the structure of **2** with those of other group 4 butadiene complexes will be presented in a later section.

The hydrogen atoms of the butadiene ligand were located; the *endo* hydrogen atoms on the terminal carbons are displaced from the butadiene carbon plane

(16) Fryzuk, M. D.; Haddad, T. S.; Berg, D. J. *Coord. Chem. Rev.* **1990**, *99*, 137−212.
(17) Krüger, C.; Barnett, B. L.; Brauer, D. In *The Organic Chemistry of Iron*; Koerner von Gustorf, E. A., Grevels, F. W., Fischler, I., Eds.; Academic Press: New York, 1978; Vol. 1, pp 17−22.
(18) Cotton, F. A.; Day, V.; Frenz, B. A.; Hardcastle, K. I.; Troup, J. M. *J. Am. Chem. Soc.* **1973**, *95*, 4522−4528.

Table 3. Bond Distances (Å) and Angles (deg) for Ti(η^4-C_4H_6)$_2$(dmpe), 4[a]

Distances			
Ti(1)−C(7)	2.277(9)	Ti(2)−C(21)	2.316(9)
Ti(1)−C(8)	2.280(9)	Ti(2)−C(22)	2.284(8)
Ti(1)−C(9)	2.289(8)	Ti(2)−C(23)	2.263(8)
Ti(1)−C(10)	2.300(8)	Ti(2)−C(24)	2.268(8)
Ti(1)−C(11)	2.325(9)	Ti(2)−C(25)	2.310(8)
Ti(1)−C(12)	2.282(9)	Ti(2)−C(26)	2.285(8)
Ti(1)−C(13)	2.269(9)	Ti(2)−C(27)	2.262(8)
Ti(1)−C(14)	2.281(10)	Ti(2)−C(28)	2.281(9)
Ti(1)−P(1)	2.547(2)	Ti(2)−P(3)	2.561(2)
Ti(1)−P(2)	2.569(2)	Ti(2)−P(4)	2.540(2)
C(7)−C(8)	1.41(1)	C(21)−C(22)	1.40(1)
C(8)−C(9)	1.37(1)	C(22)−C(23)	1.38(1)
C(9)−C(10)	1.40(1)	C(23)−C(24)	1.39(1)
C(11)−C(12)	1.41(1)	C(25)−C(26)	1.39(1)
C(12)−C(13)	1.37(1)	C(26)−C(27)	1.37(1)
C(13)−C(14)	1.40(1)	C(27)−C(28)	1.38(1)
Angles			
P(1)−Ti(1)−C(7)	93.4(3)	P(3)−Ti(2)−C(21)	88.8(2)
P(1)−Ti(1)−C(8)	119.3(3)	P(3)−Ti(2)−C(22)	116.5(2)
P(1)−Ti(1)−C(9)	111.1(2)	P(3)−Ti(2)−C(23)	112.6(2)
P(1)−Ti(1)−C(10)	77.7(2)	P(3)−Ti(2)−C(24)	80.3(2)
P(1)−Ti(1)−C(11)	83.2(2)	P(3)−Ti(2)−C(25)	84.0(2)
P(1)−Ti(1)−C(12)	111.8(2)	P(3)−Ti(2)−C(26)	112.1(2)
P(1)−Ti(1)−C(13)	146.3(3)	P(3)−Ti(2)−C(27)	146.7(2)
P(1)−Ti(1)−C(14)	146.0(2)	P(3)−Ti(2)−C(28)	147.2(2)
P(2)−Ti(1)−C(7)	83.7(2)	P(4)−Ti(2)−C(21)	82.2(2)
P(2)−Ti(1)−C(8)	113.8(2)	P(4)−Ti(2)−C(22)	110.2(2)
P(2)−Ti(1)−C(9)	147.9(2)	P(4)−Ti(2)−C(23)	145.3(2)
P(2)−Ti(1)−C(10)	145.2(2)	P(4)−Ti(2)−C(24)	147.8(2)
P(2)−Ti(1)−C(11)	89.7(2)	P(4)−Ti(2)−C(25)	90.0(2)
P(2)−Ti(1)−C(12)	116.8(2)	P(4)−Ti(2)−C(26)	117.1(2)
P(2)−Ti(1)−C(13)	111.5(3)	P(4)−Ti(2)−C(27)	111.4(2)
P(2)−Ti(1)−C(14)	78.5(3)	P(4)−Ti(2)−C(28)	79.1(3)
P(1)−Ti(1)−P(2)	74.31(7)	P(3)−Ti(2)−P(4)	74.59(7)
Displacements (Å) from the Mean C_4H_6 Planes			
H(7a)	−0.61(7)	H(21a)	−0.53(7)
H(7b)	0.00(7)	H(21b)	0.10(7)
H(8)	0.19(7)	H(22)	0.16(7)
H(9)	0.16(7)	H(23)	0.20(6)
H(10a)	0.09(7)	H(24b)	0.10(6)
H(10b)	−0.61(7)	H(24a)	−0.60(7)
H(11a)	−0.58(7)	H(25a)	−0.53(6)
H(11b)	0.19(7)	H(25b)	0.04(6)
H(12)	0.18(6)	H(26)	0.19(6)
H(13)	0.10(6)	H(27)	0.04(7)
H(14a)	−0.49(7)	H(28a)	−0.51(7)
H(14b)	0.19(8)	H(28b)	0.27(7)

[a] The corresponding parameters for molecules 1 and 2 are listed in the left and right columns, respectively.

by an average of 0.41 Å away from the titanium atom. The displacement of the *endo* hydrogen atoms reflects the twisting of the CHPh groups, which occurs to improve the bonding between the titanium center and the butadiene π-system. The hydrogen atoms attached to the interior carbon atoms are displaced 0.1 Å toward the titanium center for similar reasons.

X-ray Crystal Structure of Ti(η^4-C_4H_6)$_2$(dmpe)$_2$. Wreford has proposed that Ti(η^4-C_4H_6)$_2$(dmpe) possesses an octahedral structure similar to that of the hafnium analogue Hf(η^4-C_4H_6)$_2$(dmpe),[14] but no crystallographic study of the titanium complex has been carried out until now. Crystals suitable for examination were grown from pentane and crystallize in the space group $P\bar{1}$. Molecules of Ti(η^4-C_4H_6)$_2$(dmpe) lie on general positions but adopt near-ideal C_2 symmetry; the pseudo 2-fold axis passes through the titanium atom and the center of the C(1)−C(2) bond of the dmpe ligand. The asymmetric unit contains two independent molecules, but the corresponding bond distances and angles in the two molecules differ by less than one standard deviation in most cases and by less than two standard deviations in all cases. Crystal data are given in Table 1, and selected bond distances and angles are collected in Table 3.

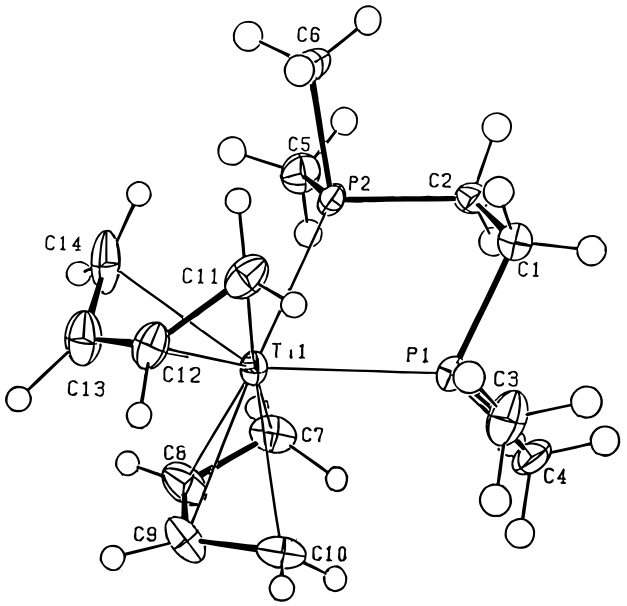

Figure 2. ORTEP diagram from the X-ray crystal structure of Ti(η^4-C_4H_6)$_2$(dmpe), **4**. The 35% probability ellipsoids are shown.

The ligands in Ti(η^4-C_4H_6)$_2$(dmpe) are disposed in an approximately octahedral fashion, Figure 2. The η^4-butadiene ligands possess essentially planar carbon skeletons and are bonded symmetrically to the titanium center. The Ti−C bond distances resemble the Hf−C distances in Hf(η^4-C_4H_6)$_2$(dmpe) after allowing for the difference in atomic radii. The distance between the titanium atom and the mean plane of the butadiene ligand of 1.795 Å is 0.15 Å shorter than that observed in the titanium(II) butadiene complex TiMe$_2$(η^4-1,4-$C_4H_4Ph_2$)(dmpe) described above. Both on steric grounds (due to the presence of the terminal phenyl substituents) and on electronic grounds (Ti^{II} should be less effective in π-back-bonding than Ti^0), the smaller distance of the titanium center from the mean butadiene plane in Ti(η^4-C_4H_6)$_2$(dmpe) is expected. The C−C bond distances within the butadiene ligand are very similar to those found in TiMe$_2$(η^4-1,4-$C_4H_4Ph_2$)(dmpe).

The hydrogen atoms of the C_4H_6 ligands have been located. The *endo* hydrogens attached to the terminal carbon atoms are displaced away from the titanium center by an average of 0.56(5) Å, whereas the *exo* hydrogens are nearly in the butadiene plane. The hydrogens attached to the interior carbon atoms are displaced an average of 0.14(7) Å toward the titanium center. As mentioned above, similar displacements of substituents out of the ligand plane have been observed for other transition metal butadiene complexes and are generally thought to be a consequence of maximizing overlap between the donor and acceptor orbitals of the diene with the appropriate d-orbitals on the metal center.

The Structures of Group 4 Butadiene Complexes. The geometry of the metal−butadiene interaction in group 4 complexes can vary significantly from complex to complex. One extreme structural motif is

(19) Erker, G.; Wicher, J.; Engel, K.; Krüger, C. *Chem. Ber.* **1982**, *115*, 3300−3310
(20) Erker, G.; Engel, K.; Krüger, C; Chiang, A.-P. *Chem. Ber.* **1982**, *115*, 3311−3323.

shown by metallocene compounds of stoichiometry $Cp_2M(\eta^4$-diene). In these complexes, the diene can adopt either a *cis* or a *trans* structure;[7,19−26] in the *cis* isomers, which are the more thermodynamically stable, the butadiene ligand possesses considerable metallacyclopentene character (structure A). At the other extreme, which is illustrated by the titanium complex $TiMe_2(\eta^4$-1,4-$C_4H_4Ph_2)$(dmpe), the butadiene ligand is bound like a true diene (structure B). Structural extremes A and B are often referred to as the σ^2,π and π,η^4 geometries, respectively. Other group 4 butadiene complexes are known that fill in the range between these two extremes.[8,14,20,27−34] The two structural parameters that have been used most often to describe the nature of the metal−butadiene geometry are (1) the dihedral angle ϕ between the mean butadiene plane and the plane containing the metal atom and the two outer (i.e., wingtip) carbon atoms[7,23,24] and (2) the difference Δd between the average metal−C(outer) and average metal−C(inner) distances.[18]

A B

Table 4 gives a listing of these structural parameters for a variety of crystallographically characterized group 4 butadiene complexes. We ask, what factors are principally responsible for dictating the metal−butadiene geometry? Although a number of molecular orbital calculations on butadiene complexes of early transition metals have been carried out,[8,24,31] no definitive answer to this question has been formulated. Fryzuk has noted that, for group 4 butadiene complexes, the π,η^4 geometry (structure B) is favored when phosphine donors are present.[28] The data in Table 4 support this observation: without exception, the 7 phosphine-ligated molecules have dihedral angles that are less than 100° and the 10 phosphine-free molecules have dihedral angles that are greater than 100°. This empirical correlation with the nature of the ancillary ligands, however, is not an explanation of the observed behavior.

Table 4. Structural Comparisons of Group 4 *cis*-Butadiene Complexes[a]

cmpd	$\phi_{dihedral}$	$d(M-C_o) - d(M-C_i)$	ref
$TiMe_2(1,4\text{-}C_4H_4Ph_2)$(dmpe)	84.9	+0.140	this work
$CpZrH(C_4H_6)$(dmpe)	88.5	0.000	30
$CpZrCl(C_4H_6)$(dmpe)	88.9	−0.006	27
$Ti(C_4H_6)_2$(dmpe)	91.9	+0.016	this work
$Hf(C_4H_6)_2$(dmpe)	94.0	−0.035	14
$HfPh(C_4H_6)$(npp)[b]	97.5	−0.193	28
$ZrPh(C_4H_6)$(npp)[b]	98.9	−0.171	28
$CpZr(C_3H_5)(C_4H_6)$		−0.103	33
$Cp^*HfCl(2,3\text{-}C_4H_4Me_2)$py	103.6	−0.204	31
$CpHf(C_3H_2Me_3)(1,2\text{-}C_4H_4Me_2)$	104.0	−0.140	29
$Cp^*HfCl(2,3\text{-}C_4H_4Me_2)$	104.2	−0.244	31
$Cp^*TiCl(1,4\text{-}C_4H_4Ph_2)$	104.3	−0.060	8
$Cp^*TiCl(C_4H_6)$	105.0	−0.101	8
$Cp^*TiCl(2,3\text{-}C_4H_4Ph_2)$	106.8	−0.260	8
$(C_5H_4Bu^t)_2Zr(C_4H_6)$	112.0	−0.191	34
$Cp_2Zr(2,3\text{-}C_4H_4Me_2)$	112.8	−0.297	32, 20
$Cp_2Hf(2,3\text{-}C_4H_4Me_2)$	116.5	−0.374	32
$Cp_2Zr(2,3\text{-}C_4H_4Ph_2)$	119.3	−0.425	20

[a] Complexes in which rings are fused to the butadiene skeleton have been excluded. The dihedral angle ϕ is defined as the angle between the mean plane of the butadiene ligand and the plane containing the metal and the outer (wingtip) cabon atoms. Angles are given in degrees and distances are given in Å. [b] npp = $N(CH_2SiMe_2PMe_2)_2$.

It has been pointed out[22,35] that the metallocene complexes cannot easily back-bond into the LUMO of a coordinated *cis*-diene because they lack a π-donating orbital in the Cp−M−Cp plane.[36] There is some evidence that larger values of ϕ result when the metal is a poorer π-donor. For example, the dihedral angles in $Cp_2Zr(\eta^4\text{-}2,3\text{-}C_4H_4Me_2)$ and $CpZrCl(\eta^4\text{-}C_4H_6)$(dmpe) are 112.8 and 88.9°, respectively.[32,27] The ν_{CO} stretching frequencies of their analogous carbonyl complexes are 1978 and 1888 cm^{-1} for $Cp_2Zr(CO)_2$[37] and 1955 and 1885 cm^{-1} for $CpZrCl(CO)_2$(dmpe);[38] these data demonstrate that the Cp_2Zr fragment is in fact the poorer π-donor. Differences in electronic factors, however, are probably not solely responsible for the wide range of dihedral angles seen in early transition metal butadiene complexes.

Silver has noted that tilting of the butadiene ligand in $CpZr(\eta^3\text{-}1,2,3\text{-}C_3H_2Me_3)(\eta^4\text{-}2,3\text{-}C_4H_4Me_2)$ minimizes the steric repulsions with other ancillary ligands and results in longer M−C distances to the inner carbon atoms of the butadiene ligand.[29] Similarly, we propose that the preferred bonding mode for butadiene complexes of the lower valent early transition metals is the π,η^4 mode (structure B) and that increasing σ^2,π character (structure A) is favored when there are significant steric repulsions between the ancillary ligands and the *meso* butadiene substituents. All of the complexes with significant σ^2,π character have either two Cp groups or one Cp* ligand that occupy considerable space in the coordination sphere of the metal center. In contrast, the dmpe ligand is rather undemanding sterically and leaves sufficient room in the coordination sphere for the butadiene ligand to adopt the preferred π,η^4 geometry.

(21) Dorf, U.; Engel, K.; Erker, G. *Organometallics* **1983**, *2*, 462−463.
(22) Erker, G.; Krüger, C.; Muller, G. *Adv. Organomet. Chem.* **1985**, *24*, 1−39.
(23) Yasuda, H.; Nakamura, A.; Kai, Y.; Nasai, N. *Topics in Physical Organometallic Chemistry*; Gielen, M. F., Ed.; Freund Publishing House Ltd.: London, 1987; Vol. 2, p 179.
(24) Yasuda, H.; Tatsumi, K.; Okamoto, T.; Mashima, K.; Lee, K.; Nakamura, A.; Kai, Y.; Kanehisa, N.; Kasai, N. *J. Am. Chem. Soc.* **1985**, *107*, 2410−2422.
(25) Yasuda, H.; Kajihara, Y.; Mashima, K.; Nagasuna, K.; Lee, K.; Nakamura, A. *Organometallics* **1982**, *1*, 388−396.
(26) Yasuda, H.; Tatsumi, K.; Nakamura, A. *Acc. Chem. Res.* **1985**, *18*, 120−125.
(27) Wielstra, Y.; Gambarotta, S. *Organometallics* **1990**, *9*, 572−577.
(28) Fryzuk, M. D.; Haddad, T. S.; Rettig, S. J. *Organometallics* **1989**, *8*, 1723−1732.
(29) Prins, T. J.; Hauger, B. E.; Vance, P. J.; Wemple, M. E.; Kort, D. A.; O'Brien, J. P.; Silver, M. E.; Huffman, J. C. *Organometallics* **1991**, *10*, 979−985.
(30) Wielstra, Y.; Meetsma, A.; Gambarotta, S. *Organometallics* **1989**, *8*, 258−259.
(31) Blenkers, J.; Hessen, B.; van Bolhuis, F.; Wagner, A. J.; Teuben, J. H. *Organometallics* **1987**, *6*, 459−469.
(32) Krüger, C.; Müller, G.; Erker, G.; Dorf, U.; Engel, K. *Organometallics* **1985**, *4*, 215−223.
(33) Erker, G.; Berg, K.; Krüger, C.; Müller, G.; Angermund, K.; Benn, R.; Schroth, G. *Angew. Chem., Int. Ed. Engl.* **1984**, *23*, 455−456.
(34) Erker, G.; Mühlenbernd, T.; Benn, R.; Rufińska, A.; Tsay, Y.-H.; Krüger, C. *Angew. Chem., Int. Ed. Engl.* **1985**, *24*, 321−323.
(35) Erker, G.; Engel, K.; Krüger, C.; Müller, G. *Organometallics* **1984**, *3*, 128−133.
(36) Lauher, J. W.; Hoffmann, R. *J. Am. Chem. Soc.* **1976**, *98*, 1729−1742 and references therein.
(37) Thomas, J. L.; Brown, K. T. *J. Organomet. Chem.* **1976**, *111*, 297−301.
(38) Wielstra, Y.; Gambarotta, S.; Roedelof, J. B.; Chiang, M. Y. *Organometallics* **1988**, *7*, 2177−2182.

Table 5. ^{1}H and ^{13}C NMR Data for the New Titanium Butadiene Complexes[a]

cmpd, temp	^{1}H NMR	assgt	^{13}C NMR
$TiMe_2(\eta^4\text{-}C_4H_6)$(dmpe), 0 °C	0.38 (s)	Ti−Me	44.1 (q, $J_{CH} = 116$)
	0.95 (br s)	PMe_2	14.0 (q, $J_{CH} = 131$)
	0.95 (br s)	PCH_2	27.0 (d, $J_{CH} = 129$)
	1.98 (δ_A)[b]	*endo*-CH_2	60.5 (t, $J_{CH} = 149$)
	2.29 (δ_B)[b]	*exo*-CH_2	
	5.92 (δ_C)[b]	CH	126.0 (d, $J_{CH} = 158$)
$TiMe_2(\eta^4\text{-}C_4H_4Ph_2)$(dmpe), 0 °C	0.32 (t, $J_{HP} = 4$)	Ti−Me	51.7 (q, $J_{CH} = 115$)
	0.64 (d, $J_{HP} = 3.0$)	PMe_2	10.5 (q, $J_{CH} = 131$)
	0.84 (d, $J_{HP} = 3.5$)	PMe_2	15.3 (q, $J_{CH} = 131$)
	0.76 (d, $J_{HP} = 12$)	PCH_2	25.7 (tt, $J_{PC} = 16$, $J_{CH} = 129$)
	3.91 (δ_A, $J_{HP} = 5$)[c]	*endo-CH*Ph	80.6 (d, $J_{CH} = 150$)
	6.07 (δ_C, $J_{HP} = 0$)[c]	CHCH	120.8 (d, $J_{CH} = 159$)
	6.91 (d, $J_{HH} = 7$)	*o*-CH	121.8 (d, $J_{CH} = 159$)
	7.13 (t, $J_{HH} = 7$)	*m*-CH	123.4 (d, $J_{CH} = 155$)
	6.84 (t, $J_{HH} = 7$)	*p*-CH	128.2 (d, $J_{CH} = 155$)
		i-C	144.6 (s)
$TiMe_2(\eta^4\text{-}C_4H_4Ph_2)$(dmpe), −110 °C	−0.78 (br s)	Ti−Me	52.8 (q, $J_{CH} = 119$)
	1.60 (br s)	Ti−Me	50.0 (q, $J_{CH} = 118$)
	0.15 (br s)	PMe_2	7.9 (q, $J_{CH} = 135$)
	0.42 (br s)	PMe_2	12.7 (q, $J_{CH} = 133$)
	0.62 (br s)	PMe_2	14.6 (q, $J_{CH} = 133$)
	0.95 (br s)	PMe_2	16.0 (q, $J_{CH} = 131$)
	d	PCH_2	24.7 (br s)[e]
	2.42 (br s)	*endo-CH*Ph	82.5 (br s)[e]
	5.02 (br s)	*endo-CH*Ph	77.0 (br s)[e]
	6.05 (br s)	CHCH	*d*
	6.39 (br s)	CHCH	*d*
	6.19 (br s)	*o*-CH	*d*
	6.85 (br s)	*p*-CH	*d*
	7.00 (br s)	*p*-CH	*d*
	7.10 (br s)	*m*-CH	*d*
	7.35 (br s)	*m*-CH	*d*
	7.45 (br s)	*p*-CH	*d*
$TiMe_2(\eta^3,\eta^1\text{-}C_8H_{12})$(dmpe), −70 °C	−1.84 (dd, $J_{PH} = 6.9$, $J_{PH} = 9.7$)	Ti−Me	32.8 (q, $J_{CH} = 105$)
	−2.18 (dd, $J_{PH} = 9.7$, $J_{PH} = 10.8$)	Ti−Me	40.3 (q, $J_{CH} = 105$)
	1.35 (s, br)	PCH_2	26.0 (dd, $J_{PC} = 12$, $J_{PC} = 18$)[e]
	1.24 (s, br)	PCH_2	27.6 (s)[e]
	1.08 (d, $J_{PH} = 7.0$)	PMe_2	12.0 (d, $J_{PC} = 7.0$)[e]
	1.06 (d, $J_{PH} = 7.5$)	PMe_2	11.0 (dd, $J_{PC} = 4.4$, $J_{PC} = 10.5$)[e]
	0.82 (d, $J_{PH} = 6.1$)	PMe_2	12.5 (dd, $J_{PC} = 3.6$, $J_{PC} = 16.4$)[e]
	0.73 (d, $J_{PH} = 5.7$)	PMe_2	13.4 (d, $J_{PC} = 10.4$)[e]
	1.32 (δ_A)[f]	CH_2	69.4 (dt, $J_{PC} = 16$, $J_{CH} = 151$)
	3.19 (δ_B)[f]		
	5.02 (δ_C)[f]	CH	126.5 (d, $J_{CH} = 150$)
	4.27 (δ_D)[f]	CH	117.2 (d, $J_{CH} = 150$)
	2.01 (δ_E)[f]	CH_2	34.3 (t, $J_{CH} = 105$)
	3.36 (δ_F)[f]		
	2.75 (δ_G)[f]	CH_2	23.9 (t, $J_{CH} = 114$)
	2.95 (δ_H)[f]		
	5.05 (δ_I)[f]	CH	107.0 (d, $J_{CH} = 158$)
	5.90 (δ_J)[f]	CH	141.2 (d, $J_{CH} = 145$)
	2.80 (δ_K)[f]	CH_2	43.0 (t, $J_{CH} = 113$)
	2.95 (δ_L)[f]		
$Ti(\eta^4\text{-}C_4H_6)_2$(dmpe), 20 °C	0.85 ("d", $^2J_{PH} + {}^3J_{PH} = 13.6$)	PMe_2	15.0 (t, $J_{PC} = 8.4$)[e]
	1.47 ("t", $^2J_{PH} + {}^5J_{PH} = 5.8$)	PCH_2	29.2 (t, $J_{PC} = 17.0$)[e]
	−0.13 (δ_A, $J_{HP} = 6.5$)[g]	*endo*-CH_2	45.7 (tt, $J_{PC} = 6.5$, $J_{CH} = 148$)
	1.57 (δ_B, $J_{HP} = 3.3$)[g]	*exo*-CH_2	
	5.54 (δ_C, $J_{HP} = 0$)[g]	CHCH	105.9 (d, $J_{CH} = 158$)

[a] Coupling constants are given in Hertz. [b] $^5J_{AA'} = 0$, $^2J_{AB} = 3.1$, $^5J_{AB'} = 0$, $^3J_{AC} = 11.2$, $^4J_{AC'} = -1.6$, $^5J_{BB'} = 0$, $^3J_{BC} = 9.1$, $^4J_{BC'} = 1.8$, $^3J_{CC'} = 7.6$. [c] $^5J_{AA'} = 0$, $^3J_{AC} = 11.6$, $^4J_{AC'} = -1.5$, $^3J_{CC'} = 8.2$. [d] Not observed. [e] Measured from the $^{13}C\{^1H\}$ spectrum. [f] $J_{AB} = 4$, $J_{BC} = 8.4$, $J_{CD} = 14.8$, $J_{DE} = 9$, $J_{EF} = 12.3$, $J_{EG} = 2$, $J_{FG} = 4$, $J_{FH} = 3$, $J_{GI} = 4$, $J_{HI} = 10$, $J_{JK} = 9$, $J_{JL} = 4$; all other coupling constants are zero or could not be established from the spectrum. [g] $^5J_{AA'} = 0$, $^2J_{AB} = 3.7$, $^5J_{AB'} = 0$, $^3J_{AC} = 10.7$, $^4J_{AC'} = -1.2$, $^5J_{BB'} = 0$, $^3J_{BC} = 9.0$, $^4J_{BC'} = 1.8$, $^3J_{CC'} = 7.3$.

Steric effects also explain why the dihedral angle ϕ is more often larger for a hafnium complex than for the corresponding zirconium complex: the smaller size[39] of Hf vs Zr makes complexes of the former metal more crowded.

Solution Structure and Dynamics of $TiMe_2(\eta^4\text{-}C_4H_4R_2)$(dmpe). ^{1}H and ^{13}C NMR data for these species (and others to be reported below) are collected in Table 5. The $^{31}P\{^1H\}$ NMR spectrum of $TiMe_2(\eta^4\text{-}C_4H_6)$(dmpe), **1**, consists of a singlet at δ 26.0 down to −90 °C; this shows that the two ends of the dmpe ligand are equivalent on the NMR time scale at this temperature. The ^{1}H NMR spectrum of **1** at −90 °C shows three broad resonances for the butadiene ligand (*endo*-CH_2, *exo*-CH_2, and *meso*-CH), one broad Ti−Me resonance, and two broad PMe resonances; this shows that the two ends of the butadiene ligand and the two Ti−Me groups are equivalent at this temperature.

If we assume that the titanium center in **1** adopts a structure similar to that of its phenyl-sustituted ana-

(39) Hunter, W. E.; Atwood, J. L.; Fachinetti, G.; Floriani, C. *J. Organomet. Chem.* **1981**, *204*, 67−74.

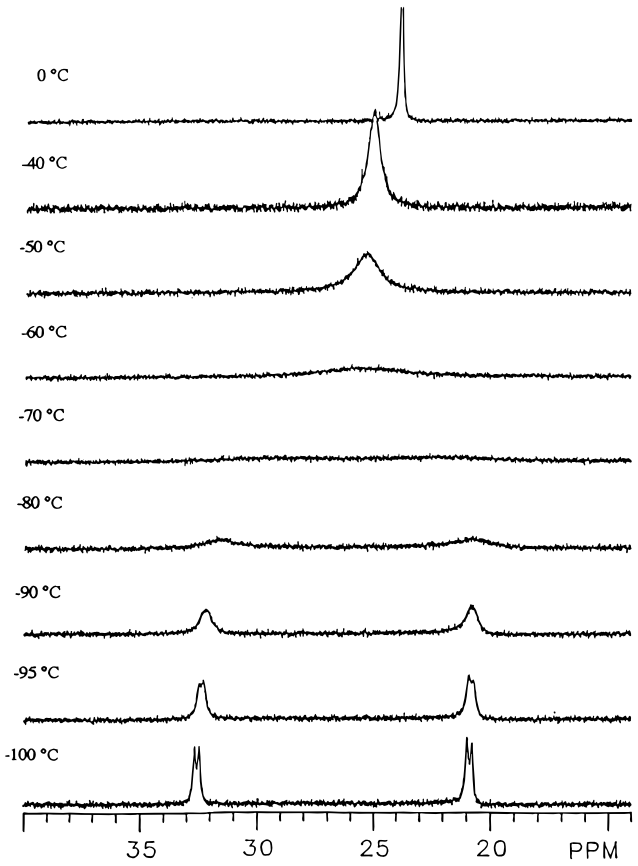

Figure 3. Variable-temperature 202 MHz $^{31}P\{^1H\}$ NMR spectra of $TiMe_2(\eta^4\text{-}1,4\text{-}C_4H_4Ph_2)$(dmpe), **2**, in toluene-d_8.

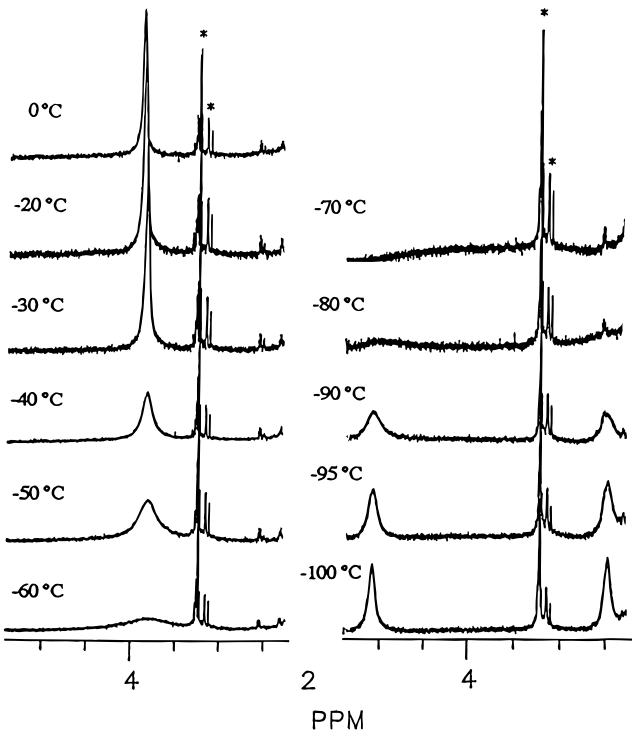

Figure 4. Variable-temperature 500 MHz ^1H NMR spectra of $TiMe_2(\eta^4\text{-}1,4\text{-}C_4H_4Ph_2)$(dmpe), **2**, in toluene-d_8; peaks due to the terminal protons of the diphenylbutadiene ligands are shown; asterisks designate peaks due to diethyl ether and other impurities.

logue **2**, then the molecule must be fluxional at −90 °C to explain why the number of resonances seen is smaller than expected. We were unable to find a solvent that would enable us to collect spectra of **1** at lower temperatures.

At higher temperatures, the ^1H and ^{31}P NMR spectra of **1** change as a result of exchange with free dmpe. The ^{31}P NMR peak broadens above −20 °C, and the two PMe resonances in the ^1H NMR spectrum coalesce into a single peak at 25 °C. At room temperature, the resonances for the bound butadiene ligand correspond to an AA′BB′CC′ spin system and have lost the couplings to the phosphorus nuclei of the dmpe ligand seen at −90 °C. A simulation of the AA′BB′CC′ pattern shows that the geminal $^2J_{HH}$ coupling constant between the methylene protons is 3.1 Hz. This coupling constant is similar to those of 1−5 Hz seen for butadiene complexes of the later transition elements[40−44] but differs from those of 7−12 Hz seen for butadiene complexes with some σ^2,π metallacyclopentene character.[8,29,31,32] The $^1J_{CH}$ coupling constants of 149 and 158 Hz for the butadiene carbons also are similar to those of late transition metal butadiene complexes but differ from those seen for most (but not all) σ^2,π butadiene species. There appears to be no strong correlation between the magnitude of the $^1J_{CH}$ coupling constants and the dihedral angle ϕ:[45] for unsubstituted butadiene complexes of the group 4 metals, the $^1J_{CH}$ coupling constants all lie between 138 and 148 Hz for the wingtip carbons and between 154 and 165 Hz for the inner carbons.

Like **1**, the 1,4-diphenylbutadiene analogue $TiMe_2(\eta^4\text{-}1,4\text{-}C_4H_4Ph_2)$(dmpe), **2**, is also a fluxional molecule but in this case the dynamic process can be frozen out at lower temperatures. The $^{31}P\{^1H\}$ NMR spectrum at −100 °C consists of two equal intensity peaks (Figure 3). The numbers of resonances observed in the ^1H and ^{13}C NMR spectra of **2** at −110 °C clearly show that in the slow exchange limit the molecule has no symmetry: two Ti−Me environments, four PMe environments, four environments for the backbone protons of the 1,4-diphenylbutadiene ligand, and two different phenyl environments for the 1,4-diphenylbutadiene ligand are seen. These observations rule out trigonal prismatic and *trans*-octahedral structures but are completely consistent with the *cis*-octahedral geometry determined crystallographically.

As the temperature is raised, coalescence processes can be observed. The two resonaces seen in the $^{31}P\{^1H\}$ NMR spectrum of **2** coalesce to a singlet, and at higher temperatures, this resonance broadens and moves upfield owing to exchange with free dmpe (Figure 3). The ^{13}C and ^1H NMR spectra show that at 0 °C the two ends of the 1,4-diphenylbutadiene ligand have now become equivalent: there is one *endo*-CH (Figure 4), one *meso*-CH, and one *exo*-phenyl environment. In addition, although the two ends of the dmpe ligand are equivalent at 0 °C, there are two different dmpe PMe environments.

(40) Crews, P. *J. Am. Chem. Soc.* **1973**, *95*, 638−640.
(41) Ruh, S.; von Philipsborn, W. *J. Organomet. Chem.* **1977**, *127*, C59−C61.
(42) Bachmann, K.; von Philipsborn, W. *Org. Magn. Reson.* **1976**, *8*, 648−654.
(43) Benn, R.; Schroth, G. *J. Organomet. Chem.* **1982**, *228*, 71−85.
(44) Tachikawa, M.; Shapley, J. R.; Haltiwanger, R. C.; Pierpont, C. G. *J. Am. Chem. Soc.* **1976**, *98*, 4651−4652.

(45) For example, the $^1J_{CH}$ coupling constants to the wingtip and inner carbon atoms of the butadiene ligands in $CpZrCl(\eta^4\text{-diene})$(dmpe) (143 and 162 Hz)[27] and $Cp_2Zr(\eta^4\text{-diene})$ (144 and 165 Hz)[32] are nearly identical despite the large difference in the dihedral angle ϕ (see Table 4).

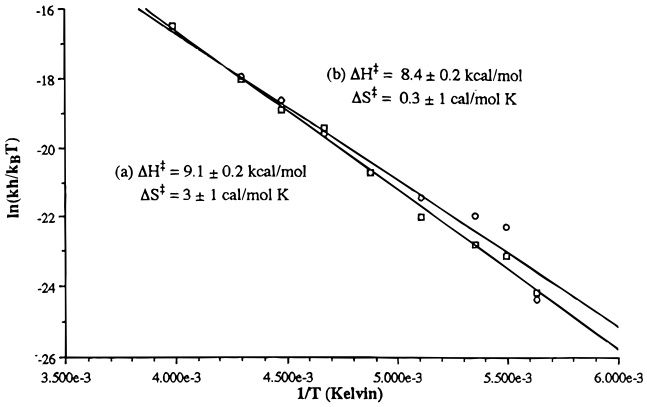

Figure 5. Eyring plots for $TiMe_2(\eta^4\text{-}1,4\text{-}C_4H_4Ph_2)$(dmpe), **2**, in toluene-d_8. The exchange rates are obtained from (a) the variable-temperature 500 MHz ^1H NMR resonances of the terminal butadiene protons (□) and (b) the variable-temperature 202 MHz $^{31}P\{^1H\}$ NMR spectra (○).

The variable-temperature $^{31}P\{^1H\}$ and ^1H NMR line shapes of **2** were used to determine the thermodynamic parameters that describe the fluxional process. The $^{31}P\{^1H\}$ NMR line shapes and the ^1H NMR line shapes of the *endo*-CH protons of the 1,4-diphenylbutadiene ligand were computer fit. The resulting rate constants as a function of temperature were used to construct Eyring plots (Figure 5). The two sets of data give essentially identical activation parameters, and thus, a single fluxional process is responsible for exchange of the two ends of the phosphine ligand and the two ends of the 1,4-diphenylbutadiene ligand. The deduced activation parameters are $\Delta H^{\ddagger} = 9.1 \pm 0.2$ kcal mol^{-1} and $\Delta S^{\ddagger} = 3 \pm 1$ cal mol^{-1} K^{-1}. The small entropy of activation is consistent with an intramolecular exchange process. Similar but less accurate activation parameters were derived from analyses of the variable-temperature ^1H NMR line shapes of the *meso* butadiene protons (which decoalesced only below −90 °C) and the PMe_2 and Ti−Me groups (which obscured each other near their coalescence temperatures of ca. −85 and −70 °C, respectively).

Two mechanisms have been invoked to account for the variable-temperature spectra of other butadiene complexes of the group 4 elements: the envelope-flip mechanism and diene rotation. Neither of these mechanisms would exchange the two Ti−Me groups, the two ends of the 1,4-diphenylbutadiene ligand, or the two ends of the dmpe ligand in **2**.[46] Therefore, these mechanisms can be ruled out.

One intramolecular exchange mechanism that is consistent with the dynamic NMR spectra we observe is a trigonal-twist mechanism (also called a Bailar twist).[47−49] This mechanism exchanges the two Ti−Me groups and the two ends of the dmpe and butadiene ligands, but the methyl groups on each end of the phosphine ligand remain diastereotopic: these four groups are exchanged in a *pairwise* fashion, as shown by the presence of a mirror plane that relates the two triangular faces of the trigonal prismatic transition structure. Trigonal twists have been proposed to be responsible for the fluxional nature of other six-coordinate butadiene complexes, such as the d^6 chromium species $Cr(\eta^4\text{-diene})(CO)_4$.[50]

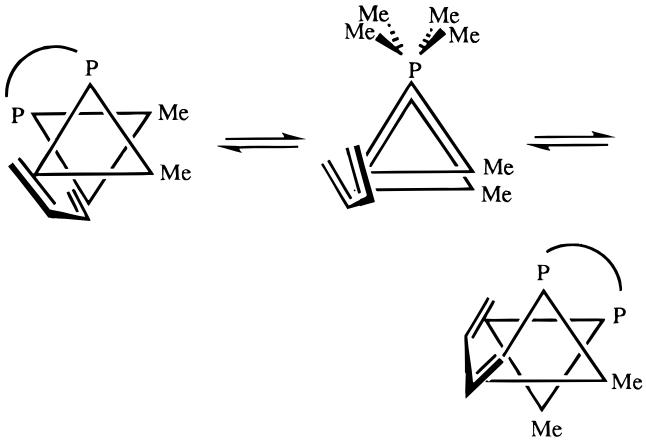

We cannot, however, rule out the possibility that the fluxionality of **1** and **2** involves the formation of five-coordinate structures by dissociation of one arm of one of the chelating ligands. The resulting five-coordinate intermediate has many degrees of freedom, however, and only certain of the available rearrangement pathways would exchange the Ti−Me groups and the two ends of the butadiene ligand without exchanging the diastereotopic PMe_2 groups. Interestingly, the pseudorotations that can account for the observed exchange processes closely resemble those of a trigonal twist in which one end of a phosphine ligand has become detached.[51]

Solution Structure of the Titanium(0) Butadiene Complex $Ti(\eta^4\text{-}C_4H_6)_2$(dmpe). The NMR spectra of $Ti(\eta^4\text{-}C_4H_6)_2$(dmpe) are in general agreement with previous descriptions:[9] there are three environments (*exo*-CH_2, *endo*-CH_2, and *meso*-CH) for the butadiene protons and only one environment for the phosphorus-bound methyl groups. The spectra are essentially unchanged between −80 and 0 °C, except that the resonances broaden slightly at lower temperatures due to slowing of a fluxional process and the onset of decoalescence (see below). The second-order coupling patterns for the butadiene ligands in the ^1H NMR spectrum were not analyzed previously, and therefore, we simulated the spectrum to deduce the coupling constants. The derived chemical shifts and coupling constants are collected in Table 5. The H−H coupling constants in **4** are nearly identical to those of the butadiene ligand in the titanium(II) complex $TiMe_2(\eta^4\text{-}C_4H_6)$(dmpe).

As Wreford has pointed out,[9] the simplicity of the NMR spectrum of **4** indicates that a fluxional process is occurring that renders the two ends of the butadiene ligands and the two ends of the phosphine ligands equivalent. This behavior is again inconsistent with both the envelope-flip mechanism and the butadiene rotation mechanism; neither of these processes would effect these site exchanges. As before, a dynamic

(46) In fact, no complex of a 1,4-disubstituted butadiene has been observed to undergo the envelope-flip process. Evidently, such a motion is prevented by unfavorable steric interactions in the metallacyclopentane transition state.[28]

(47) Bailar, J. C. *J. Inorg. Nucl. Chem.* **1958**, *8*, 165−175.

(48) Springer, C. S.; Sievers, R. E. *Inorg. Chem.* **1967**, *6*, 852−854.

(49) Butadiene rotations and trigonal twists are mechanistically indistinguishable in five-coordinate $M(\eta^4\text{-diene})L_3$ complexes, see: Warren, J. D.; Clark, R. J. *Inorg. Chem.* **1970**, *9*, 373−379. Van Catledge, F. A.; Ittel, S. D.; Jesson, J. P. *J. Organomet. Chem.* **1979**, *168*, C25−C29.

(50) Kotzian, H.; Kreiter, C. G.; Özkar, S. *J. Organomet. Chem.* **1982**, *229*, 29−42.

(51) A referee suggested that for **2** the fluxional mechanism may involve equilibration with an isomer in which the open edge of the butadiene ligand is oriented toward a Ti−Me bond rather than a Ti−P bond. We see no evidence of this second isomer, however.

process that can account for the fluxionality of this molecule is the trigonal-twist mechanism. The exchange process can also be explained in terms of a five-coordinate intermediate. In the Appendix, we consider

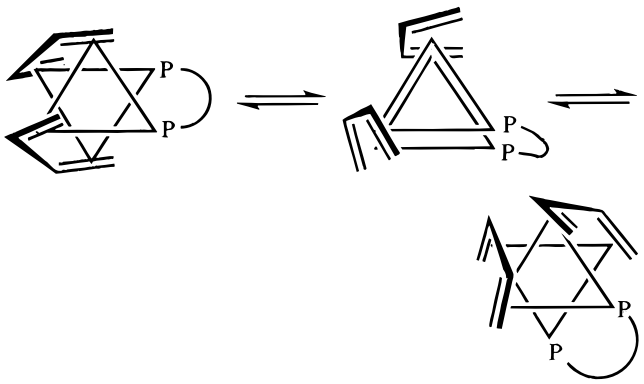

whether trigonal twists might also be consistent with the dynamic processes seen for other group 4 butadiene complexes.

Solution Structure of the Titanium(IV) "Bis(butadiene)" Complex $TiMe_2(\eta^3,\eta^1\text{-}C_8H_{12})$(dmpe). The ^1H, $^{13}C\{^1H\}$, and $^{31}P\{^1H\}$ NMR spectra of the product obtained from the reaction of $TiMe_2(dmpe)_2$ with excess butadiene for prolonged periods at −20 °C show it to be one species with a stoichiometry of $TiMe_2(C_8H_{12})$(dmpe), **3**. The two Ti−Me groups in **3** are chemically inequivalent and appear at δ −1.84 (dd, J_{PH} = 6.9, 9.7 Hz) and −2.18 (dd, J_{PH} = 9.7, 10.8 Hz) in the ^1H NMR spectrum at −70 °C (Figure 6); each resonance appears as a doublet of doublets due to coupling with the two ^{31}P nuclei of the dmpe ligand (as shown by selectively decoupled $^1H\{^{31}P\}$ NMR experiments). The low-temperature $^{31}P\{^1H\}$ NMR spectrum contains two singlets of equal intensity (δ 28.5, 34.2), which shows that the two ends of the dmpe ligand are chemically inequivalent. The J_{PP} coupling is essentially zero.

The identity of the C_8H_{12} ligand in **3** has been established from a combination of one-dimensional ^1H, $^1H\{^1H$ selective}, and ^{13}C NMR experiments and from two-dimensional $^1H-^1H$ COSY and $^1H-^{13}C$ HETCOR experiments at −70 °C. The spectra reveal that the C_8H_{12} fragment is a linear C_8 chain consisting of two butadiene ligands joined end-to-end: $CH_2CHCHCH_2-CH_2CHCHCH_2$. The bonding between the C_8 chain and the titanium center was established from the $^1J_{CH}$ coupling constants and ^{13}C chemical shifts (Table 5). The first three carbon atoms in the chain and the sixth and seventh carbon atoms have $^1J_{CH}$ coupling constants that are near 150 Hz, whereas the remaining carbon atoms have $^1J_{CH}$ coupling constants of less than 130 Hz. This pattern is most consistent with a structure in which the titanium is bonded to the first three carbons in a π-allylic fashion and to the eighth carbon in a σ fashion; the sixth and seventh carbon atoms are connected by a double bond that is not interacting with the titanium atom.

The ^1H and $^{13}C\{^1H\}$ NMR chemical shifts generally follow the same pattern seen for group 10 complexes with the same η^3,η^1-octa-1,6-diene-1,8-diyl ligand.[52−54] Nakamura has isolated several zirconium and hafnium complexes with similar octadienediyl ligands by treatment of $Cp_2Zr(\eta^4$-diene) or $Cp_2Hf(\eta^4$-diene) with excess diene.[7,55] Schrock has reported the formation of a similar ligand by the interaction of butadiene with $Zr_2Cl_6(PEt_3)_4$; the complex $ZrCl_2(C_8H_{12})(PEt_3)$ is formed, and the spectroscopic evidence suggests that the C_8H_{12} ligand is coordinated as a bis(allyl).[56] The zirconium complex $(C_8H_8)Zr(\eta^3,\eta^3\text{-}C_{10}H_{16})$, in which the decadienediyl ligand was generated by coupling of two 1,3-pentadiene molecules, has been crystallographically characterized.[57]

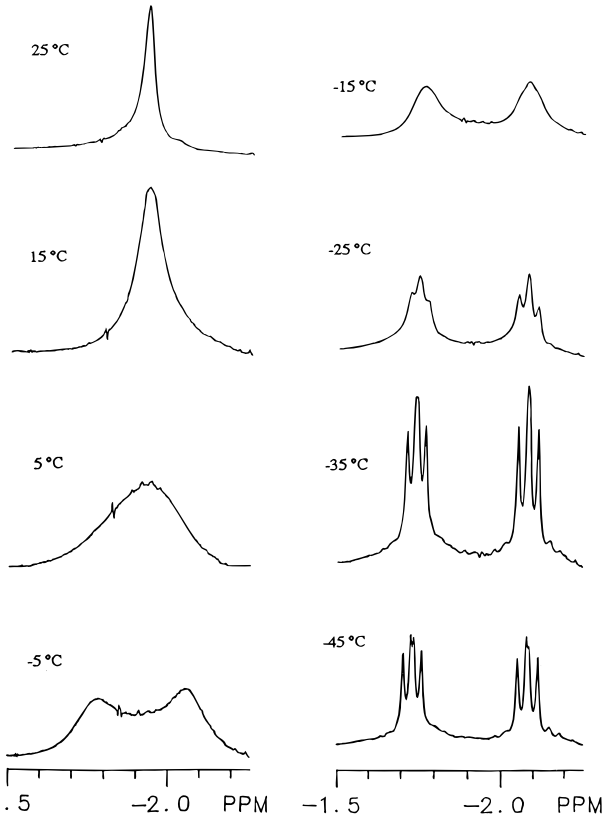

Figure 6. Variable-temperature 300 MHz ^1H NMR resonances of the Ti−Me groups in $TiMe_2(\eta^3,\eta^1\text{-}C_8H_{12})$(dmpe), **3**. The apparently more rapid broadening of the downfield Ti−Me resonance and the asymmetry in the line shape near the coalescence point are consequences of the differing J_{HP} couplings to the two Ti−Me groups and are exactly reproduced in the simulations obtained from the program DNMR3.

Variable-temperature NMR spectra show that **3** is involved in a dynamic process. The two inequivalent Ti−Me groups seen at −50 °C broaden at higher temperatures and coalesce at 5 °C (Figure 6). Similar broadening and coalescence is seen in the $^{31}P\{^1H\}$ NMR spectrum. The proton resonances of the octadienediyl ligand also broaden as the temperature is increased, but decomposition occurs before the coalescence point can be reached.

The dynamic process which exchanges the titanium methyl protons, the phosphorus nuclei, and the octadi-

(52) Benn, R.; Büssemeier, B.; Holle, S.; Jolly, P. W.; Mynott, R.; Tkatchenko, I.; Wilke, G. *J. Organomet. Chem.* **1985**, *270*, 63−86.
(53) Buch, H. M.; Schroth, G.; Mynott, R.; Binger, P. *J. Organomet. Chem.* **1983**, *247*, C63−C65.
(54) Baker, G. K.; Green, M.; Howard, J. A. K.; Spencer, J. L.; Stone, F. G. A. *J. Chem. Soc., Dalton Trans.* **1978**, 1839−1847.
(55) Kai, Y.; Kanehisa, N.; Miki, K.; Kasai, N.; Mashima, K.; Nagasuna, K.; Yasuda, H.; Nakamura, A. *Chem. Lett.* **1982**, 1979−1982.
(56) Wengrovius, J. H.; Schrock, R. R.; Day, C. S. *Inorg. Chem.* **1981**, *20*, 1844−1849.
(57) Brauer, D. J.; Krüger, C. *Organometallics* **1982**, *1*, 207−210.

Scheme 1

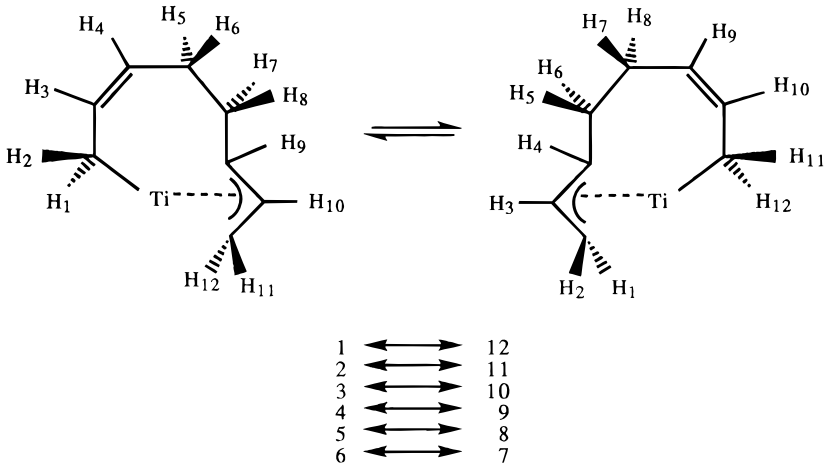

enediyl protons is an oscillatory movement that exchanges the η^1 and η^3 points of attachment of the octadienediyl ligand. Scheme 1 illustrates which pairs of protons in the octadienediyl ligand are exchanging.

The rate of the dynamic process as a function of temperature has been determined by simulating the line shapes of the Ti−Me groups of **3**. The program DNMR3H was used to simulate the exchange process of an A_3B_3XY spin system where A and B are the titanium methyl protons and X and Y are the two phosphorus nuclei of the dmpe ligand. Since there is no coupling between the A and B protons and because there are no magnetically inequivalent but chemically equivalent nuclei, the simulation was repeated using a ABXY spin system. This gave identical results except that the times needed to carry out the calculations of the line shapes were considerably shorter.

An Eyring plot was constructed from the rate and temperature data (Figure 7), and activation parameters were calculated. The activation parameters are $\Delta H^{\ddagger} = 13.6 \pm 0.5$ kcal mol^{-1} and $\Delta S^{\ddagger} = 2 \pm 2$ cal mol^{-1} K^{-1}; the small value of the activation entropy confirms that the exchange process is intramolecular.

Catalytic Dimerization of Butadiene. When a toluene solution of $TiMe_2(dmpe)_2$ is treated with ca. 25 equiv of butadiene in an NMR tube at −78 °C and then warmed to 25 °C, the solution color changes from dark-red to green. Over 24 h at 25 °C, butadiene is catalytically dimerized to 4-vinylcyclohexene, which is the only organic product observable by ^{13}C NMR spectroscopy. At 25 °C, the rate of dimerization of butadiene catalyzed by $TiMe_2(dmpe)_2$ is ∼4 turnovers/h. For comparison,

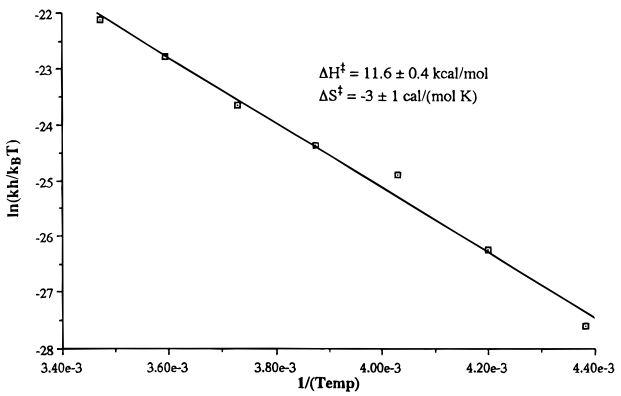

Figure 7. Eyring plot of the rates of methyl group exchange in $TiMe_2(\eta^3,\eta^1\text{-}C_8H_{12})$(dmpe), **3**, in toluene-d_8.

Scheme 2

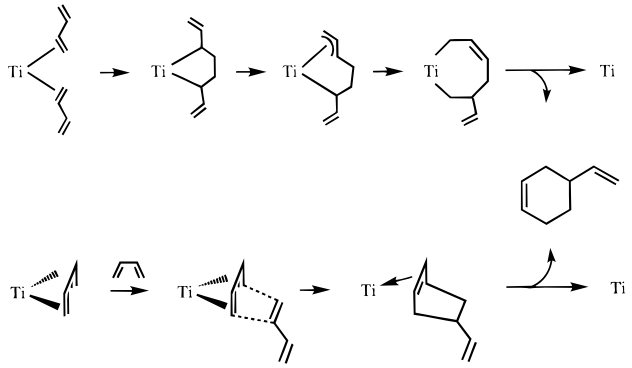

the thermal dimerization of butadiene to 4-vinylcyclohexene occurs at significant rates only above 150 °C.[3] A control experiment conducted in an NMR tube in the absence of $TiMe_2(dmpe)_2$ confirmed that butadiene does not spontaneously dimerize to any observable extent in solution over 24 h at 25 °C.

At least two mechanisms can be drawn for the catalytic dimerization of 1,3-butadiene to 4-vinylcyclohexene: (1) a metal-promoted [2 + 4] Diels−Alder addition in which free butadiene acts as a dienophile and a coordinated η^4-butadiene ligand serves as the activated diene or (2) a metallacyclic mechanism similar to that responsible for the dimerization of mono(enes) (Scheme 2). This latter pathway would involve the coupling of two butadienes to form initially a 1,4-divinyltitanacyclopentane species; subsequent allylic rearrangement would generate a vinyltitanacycloheptene ring, which could reductively eliminate to give 4-vinylcyclohexene. The two mechanisms are impossible to distinguish from labeling studies since in neither case are C−H or C−C bonds broken.

The isolation and structural characterization of $TiMe_2(\eta^3,\eta^1\text{-}C_8H_{12})$(dmpe), **3**, suggests that the latter mechanism is the operative one, however. This organometallic species is evidently the intermediate that is formed immediately before liberation of 4-vinylcyclohexene in the catalytic cycle. As we have mentioned above, complex **3** converts to 4-vinylcyclohexene and the mono(butadiene) adduct **1** at temperatures above −20 °C and in the presence of excess butadiene.

We note that the mechanism proposed is very similar

(58) Brenner, W.; Heimbach, P.; Hey, H.; Müller, E. W.; Wilke, G. *Liebigs Ann. Chem.* **1969**, *727*, 161−182.

to that originally proposed by Wilke to account for the catalytic dimerization of butadiene by nickel catalysts.[58]

It is not entirely clear why the titanium(II) complex $TiMe_2(dmpe)_2$ is able to cyclodimerize butadiene while other homogeneous early transition metal catalysts such as Cp_2M(diene) afford linear dimers.[7−11] The different products reflect the fact that the vinyltitanacycloheptene intermediate generated from $TiMe_2(dmpe)_2$ readily undergoes reductive elimination with formation of a C−C bond, whereas similar intermediates with other ancillary ligands do not. Linear butadiene dimers can only be formed if a C−H bond is broken; evidently, this C−H bond breaking step (or some subsequent step) is slow relative to C−C reductive elimination for the metallacyclic intermediates generated from $TiMe_2(dmpe)_2$ but fast in other systems.

Finally, we note that most *heterogeneous* butadiene dimerization catalysts based on early transition metals also generate linear octatriene products,[2,4] but there have been two reports in the patent literature of heterogeneous titanium-based catalysts that effect the dimerization of butadiene to 4-vinylcyclohexene.[59,60]

Concluding Remarks

Two different organometallic products have been isolated from the reaction of $TiMe_2(dmpe)_2$ and butadiene: the titanium(II) butadiene complex $TiMe_2(\eta^4\text{-}C_4H_6)$(dmpe) is formed initially, and the titanium(IV) η^3,η^1-octa-1,6-diene-1,8-diyl complex $TiMe_2(\eta^3,\eta^1\text{-}C_8H_{12})$(dmpe) is formed after prolonged exposure to excess butadiene. The reaction of $TiMe_2(dmpe)_2$ with butadiene also results in the catalytic dimerization of the diene to 4-vinylcyclohexene at rates of 4 turnovers/h at 25 °C. We have proposed a specific mechanism for the catalytic dimerization chemistry that is based on the identities of the organometallic species isolated from the reaction mixture and from analogous studies of the reactions of $TiMe_2(dmpe)_2$ with other alkenes.[12] The proposed mechanism involves the following steps: (1) displacement of a dmpe ligand and coordination of two diene ligands to the metal center, (2) coupling of the coordinated diene ligands to form a divinyltitanacyclopentane complex, (3) allylic rearrangement to a vinyltitanacycloheptene complex, and (4) reductive elimination of 4-vinylcyclohexene. Reactions analogous to the first two steps in this sequence also take place when $TiMe_2(dmpe)_2$ reacts with alkenes such as ethylene, propene, and styrene; however, in these cases, the metallacyclopentane intermediate cannot undergo an allylic rearrangement and instead β-eliminates to form a titanium(IV) butenyl hydride complex.[12] Interestingly, the titanium-bound methyl groups are spectators throughout the catalytic cycle.

One interesting aspect of the pseudo-octahedral molecules $TiMe_2(\eta^4\text{-}C_4H_4R_2)$(dmpe) and $Ti(\eta^4\text{-}C_4H_6)_2$(dmpe) described above is that they are fluxional, and the variable-temperature NMR spectra of these molecules are consistent with an exchange mechanism that passes through a trigonal prismatic (or five-coordinate) structure. For these d^2 and d^4 molecules, the activation energies for the fluxional process are relatively small: for example, $\Delta H^{\ddagger} = 9.1 \pm 0.2$ kcal mol^{-1} and $\Delta S^{\ddagger} = 3 \pm 1$ eu for the 1,4-diphenylbutadiene complex.

Lastly, we have suggested an explanation for the unusually wide range of bonding modes seen for early transition metal butadiene complexes. The dihedral angle ϕ (defined as the angle between the mean butadiene plane and the plane defined by the metal center and the outer carbon atoms of the butadiene ligand) varies from a minimum of 84.9° for $TiMe_2(1,4\text{-}C_4H_4Ph_2)$(dmpe) to a maximum of 119.3° for $Cp_2Zr(2,3\text{-}C_4H_4Ph_2)$. We suggest that the principal factor that dictates the structure is steric repulsions between the substituents on the inner carbon atoms of the butadiene ligand and the other ancillary ligands about the metal center; electronic factors play a lesser role.

Experimental Section

All operations were carried out under vacuum or under argon. Solvents were distilled under nitrogen from sodium (toluene) or sodium−benzophenone (pentane, diethyl ether) immediately before use. The titanium(II) alkyl $TiMe_2(dmpe)_2$ was prepared as described elsewhere.[13] 1,3-Butadiene (Aldrich), 1,4-diphenyl-1,3-butadiene (Aldrich), and triethylaluminum (Ethyl) were used as received.

Microanalyses were performed by the University of Illinois Microanalytical Laboratory. The IR spectra were recorded on a Perkin-Elmer 599B instrument as Nujol mulls between KBr plates. The ^{1}H and ^{13}C NMR spectra were recorded on General Electric QE-300, General Electric GN-500, and Varian Unity-400 instruments, and the ^{31}P NMR spectra were recorded on General Electric GN-300NB and Varian Unity-400 spectrometers. Chemical shifts are reported in δ units (positive chemical shifts to higher frequency) relative to $SiMe_4$ (^{1}H, ^{13}C) or H_3PO_4 (^{31}P). All peak integrals are consistent with the assignments and are therefore omitted. Melting points were determined on a Thomas−Hoover Unimelt apparatus in closed capillaries under argon.

Simulations of the dynamic NMR spectra were carried out using the program DNMR, which is available from the Quantum Chemistry Program Exchange. The rates of exchange as a function of temperature were determined from visual comparisons of experimental spectra with computed trial line shapes. The errors in the rate constants of ca. 5% were estimated on the basis of subjective judgments of the sensitivities of the fits to changes in the rate constants. The temperature of the NMR probe was calibrated using a methanol temperature standard, and the estimated error in the temperature measurements was 1 K. The activation parameters were calculated from an unweighted nonlinear least-squares procedure contained in the program Passage, which is available from Passage Software Inc. The errors in the activation parameters were computed from error propagation formulas derived from the Eyring equation.[61]

Dimethyl(η^4-butadiene)[1,2-bis(dimethylphosphino)ethane]titanium(II), 1. A solution of $TiMe_2(dmpe)_2$ (0.20 g, 0.53 mmol) in pentane (50 mL) was cooled to −72 °C, and 1,3-butadiene (0.22 L, 10 mmol) was condensed in. The solution turned green as it was warmed to −20 °C. After the solution had been stirred at −20 °C for 30 min, the solvent was removed under vacuum at 25 °C and the resulting greenish-blue oil was extracted with pentane (3 × 30 mL). The combined extracts were filtered, concentrated to ca. 5 mL, and cooled to −20 °C for 24 h to afford a green oil. The oily nature of the product made it difficult to establish an accurate yield; however, sealed-tube NMR experiments show that this product is formed in >90% high yield under the reaction conditions cited. The NMR spectra of the isolated green oil show that it contains

(59) Wilson, R. A. L.; Pugh, L. K. Brit. Patent 1 105 589, 1977; *Chem. Abstr.* **1968**, *68*, 77849v.
(60) Mori, H.; Imaizumi, F.; Shigetoshi, H. Jpn. Patent 77-08 022, 1977; *Chem. Abstr.* **1977**, *87*, 40079k.
(61) Morse, P. M.; Spencer, M. D.; Wilson, S. R.; Girolami, G. S. *Organometallics* **1994**, *13*, 1646−1655.

some free dmpe and traces of $Ti(C_4H_6)_2$(dmpe). $^{31}P\{^1H\}$ NMR (toluene-d_8, 0 °C): δ 26.0 (s).

Dimethyl(η^4-*trans,trans*-1,4-diphenyl-1,3-butadiene)-[1,2-bis(dimethylphosphino)ethane]titanium(II), 2. To a mixture of $TiMe_2$(dmpe)$_2$ (0.39 g, 1.0 mmol) and 1,4-diphenyl-1,3-butadiene (0.26 g, 1.0 mmol) at −40 °C was added diethyl ether (30 mL). After the solution had been stirred at 0 °C for 4 h, the solution color was brown-green and a brown precipitate had formed. The solvent was removed at 0 °C under vacuum. While the temperature of the flask was kept at 0 °C, the resulting solid was washed once with pentane (50 mL) and then was extracted with diethyl ether (50 mL). The extract was filtered, concentrated to ca. 10 mL, and cooled to −20 °C to afford dichroic red-green crystals. Yield: 0.10 g (40%). Anal. Calcd: C, 66.4; H, 8.35; Ti, 11.0. Found: C, 65.1; H, 8.35; Ti, 11.3. Mp: 94 °C (dec). $^{31}P\{^1H\}$ NMR (toluene-d_8, 0 °C): δ 25.5 (br s). $^{31}P\{^1H\}$ NMR (toluene-d_8, −110 °C): δ 20.5 (d, $^2J_{PP}$ = 36 Hz), 32.0 (d, $^2J_{PP}$ = 36 Hz). IR (cm^{-1}): 3060 (w), 3020 (w), 1935 (w), 1581 (s), 1490 (s), 1455 (m), 1445 (m), 1415 (m), 1375 (m), 1320 (m), 1395 (m), 1200 (s), 1175 (m), 1150 (w), 1125 (w), 1070 (w), 1020 (w), 990 (w), 945 (m), 935 (m), 930 (m), 885 (m), 825 (w), 760 (m), 745 (m), 730 (m), 700 (s), 645 (w), 520 (m), 468 (m), 428 (m).

Dimethyl(η^3,η^1-*trans,trans*-octa-2,6-diene-1,8-diyl)[1,2-bis(dimethylphosphino)ethane]titanium(IV), 3. To a solution of $TiMe_2$(dmpe)$_2$ (0.30 g, 0.89 mmol) in pentane (10 mL) at −72 °C was added excess 1,3-butadiene (0.10 L, 4.6 mmol) from a calibrated gas manifold. The flask was filled with argon, sealed, and allowed to stand for 24 h at −20 °C. Over this period, the solution first became green-blue and then brown. The solvent was removed under vacuum at −72 °C to afford an orange solid.

If the solvent is removed at −20 °C instead of at −72 °C, some of the product (about 20% depending on the exact conditions) is converted into the titanium(II) butadiene complex $TiMe_2(\eta^4$-$C_4H_6)$(dmpe).

Bis(η^4-butadiene)[1,2-bis(dimethylphosphino)ethane]-titanium(0), 4. A solution of $TiMe_2$(dmpe)$_2$ (0.15 g, 0.40 mmol) in diethyl ether (30 mL) was cooled to −72 °C, and 1,3-butadiene (ca. 0.15 L, 6.5 mmol) was condensed in. Triethylaluminum (0.14 g, 1.2 mmol) was added, and then the solution was warmed to 25 °C over 4 h; during this period, the solution color turned green and then blue. The solvent was removed under vacuum, and the resulting solid was extracted with pentane (30 mL). This filtered extract was concentrated to ca. 5 mL and cooled to −20 °C to afford crystals of the product. Yield: 0.11 g (92%). $^{31}P\{^1H\}$ NMR (toluene-d_8, 20 °C): δ 38.2 (s).

Catalytic Dimerization of Butadiene to 4-Vinylcyclohexene. A solution of $TiMe_2$(dmpe)$_2$ (0.07 g, 0.18 mmol) in toluene-d_8 (1.0 mL) in a 5 mm o.d. NMR tube was cooled to −78 °C, and butadiene (ca. 0.1 L, 4.5 mmol) was condensed in. The NMR tube was flame sealed. The reaction was monitored by ^1H, ^{13}C, and ^{31}P NMR spectroscopy; the ^{13}C NMR spectra were most useful for following the catalysis. Over the course of 24 h at 25 °C, the ^{13}C NMR peaks due to butadiene at δ 137.0 and 117.6 diminished and new peaks at δ 143.9, 126.8, 126.1, 112.3, 38.0, 31.5, 28.6, and 25.2 grew in. All of these peaks are assignable to 4-vinylcyclohexene; the only other peak detectible in the spectrum was due to dmpe. A similar experiment in the absence of $TiMe_2$(dmpe)$_2$ showed that no detectible dimerization occurred over 24 h.

Crystallographic Studies.[62] Single crystals of $TiMe_2(\eta^4$-1,4-$C_4H_4Ph_2)$(dmpe), **2**, grown from pentane/diethyl ether, were mounted on glass fibers with Paratone-N oil (Exxon) and immediately cooled to −75 °C in a cold nitrogen gas stream on the diffractometer. [Single crystals of $Ti(\eta^4$-$C_4H_6)_2$(dmpe), **4**, grown from pentane, were treated similarly. Subsequent comments in brackets will refer to compound **4**.] The overall diffraction pattern was weak. The nitrogen flow failed, causing crystal movement during the collection of the third shell; full intensity was not recovered so that data for the last part of shell 3 (259 reflections total) were corrected by a scale factor of 1.191 59. Standard peak search and indexing procedures gave rough cell dimensions, and the diffraction symmetry was confirmed by inspection of the axial photographs. Least-squares refinement using 25 reflections yielded the cell dimensions given in Table 1.

Data were collected in one quadrant of reciprocal space ($\pm h$, $-k$, $+l$) by using the measurement parameters listed in Table 1. Systematic absences for $h0l$ ($h + l \neq 2n$) and $0k0$ ($k \neq 2n$) were consistent only with the space group $P2_1/n$. [For **4**, the monoclinic unit cell was consistent with the space groups $P1$ and $P\bar{1}$. The average values of the normalized structure factors suggested the choice $P\bar{1}$, which was confirmed by successful refinement of the proposed model.] The measured intensities were reduced to structure factor amplitudes and their esd's by correction for background, scan speed, Lorentz and polarization effects. Crystal decay corrections were applied (see above), and absorption corrections were applied, the maximum and minimum transmission factors being 0.970 and 0.868. [For **4**, no decay correction was needed, but an absorption correction was applied with maximum and minimum transmission factors of 0.901 and 0.832.] Systematically absent reflections were deleted, and symmetry equivalent reflections were averaged to yield the set of unique data. Only those data with $I > 2.58\sigma(I)$ were used in the least-squares refinement.

The structure was solved by direct methods (SHELX-86); correct positions for all non-hydrogen atoms were deduced from an *E*-map. Subsequent least-squares refinement and difference Fourier calculations revealed the positions of the hydrogen atoms. All remaining hydrogen atoms were included as fixed contributors in idealized positions. [For **4**, the correct positions for the titanium and phosphorus atoms were deduced from an *E*-map. Subsequent least-squares refinement and difference Fourier calculations revealed positions for all the remaining non-hydrogen and butadiene hydrogen atoms. The hydrogen atoms on the phosphine ligand did not surface and were fixed in idealized positions with C−H = 0.96 Å.] The quantity minimized by the least-squares program was $\sum w(|F_o| - |F_c|)^2$, where $w = 1.46/(\sigma(F_o)^2 + pF_o^2)$. [For **4**, $w = 1.20/(\sigma(F_o)^2 + pF_o^2)$.] The analytical approximations to the scattering factors were used, and all structure factors were corrected for both real and imaginary components of anomalous dispersion. In the final cycle of least-squares refinement, anisotropic thermal coefficients were refined for the non-hydrogen atoms and a common isotropic thermal parameter was varied for the hydrogen atoms. No correction due to extinction was necessary. [For **4**, anisotropic thermal coefficients were refined for the non-hydrogen atoms, and a common group isotropic thermal parameter was refined for the hydrogen atoms. An isotropic extinction parameter was also refined to a final value of $7(2) \times 10^{-8}$.] Successful convergence was indicated by the maximum shift/error of 0.062 [0.002] for the last cycle. Final refinement parameters are given in Table 1. The final difference Fourier map had no significant features. A final analysis of variance between observed and calculated structure factors showed no systematic errors.

(62) For details of the crystallographic procedures and programs used, see: Jensen, J. A.; Wilson, S. R.; Girolami, G. S. *J. Am. Chem. Soc.* **1988**, *110*, 4977−4982.

Appendix

Does the Trigonal-Twist Mechanism Operate in Other Group 4 Butadiene Complexes? Fryzuk has described the variable-temperature NMR spectra of several zirconium and hafnium complexes of stoichiometry $MX(C_4H_6)[N(SiMe_2CH_2PR_2)_2]$, where X was either Cl or Ph and the R groups on phosphorus were either Me or i-Pr.[28] X-ray diffraction studies showed that the $N(SiMe_2CH_2PR_2)_2$ ligand occupies a meridional configuration in these complexes. At low temperatures, there are two environments for the phosphorus nuclei and

Scheme 3

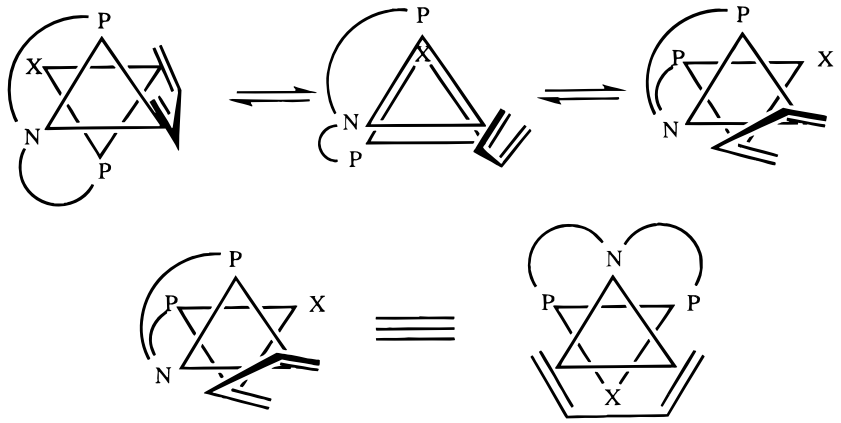

four for the carbon atoms of the butadiene ligand. At high temperatures, there is one environment for the phosphorus nuclei and two for the carbon atoms of the butadiene ligand. The envelope-flip mechanism cannot account for the appearance of the spectra at high temperatures, since this mechanism does not exchange the butadiene carbon environments. Instead, Fryzuk proposed a butadiene rotation mechanism, which is in fact consistent with the changes seen in the NMR spectrum. We point out, however, that there are no other documented cases of a six-coordinate butadiene complex that undergoes a butadiene rotation of this kind.

Fryzuk pointed out that a *mer* to *fac* isomerization of the amidophosphine ligand can also explain the exchange phenomena seen in the $MX(C_4H_6)[N(SiMe_2CH_2PR_2)_2]$ complexes.[28] This isomerization is equivalent to a trigonal twist, Scheme 3. In the *fac* configuration, there is a mirror plane that passes through the nitrogen atom of the amidophosphine ligand, the X group, and the midpoint of the butadiene ligand. This mirror plane effects the pairwise exchange of the two ends of the phosphine and butadiene ligand, as seen in the NMR studies. Consistent with the experimental results, there will be two phosphorus methyl and two silylmethyl environments in the high temperature limit because these groups remain diastereotopic in the *fac* configuration: the only molecular symmetry element in this structure, the mirror plane, relates the two arms of the amidophosphine ligand to each other but does not relate the two PMe (or SiMe) groups within each arm.

Fryzuk excluded the trigonal-twist mechanism on two grounds: first, by pointing out that the activation free energies should be sensitive to the nature of the substituents on the phosphorus atoms. This statement is certainly true, but we do not see any *a priori* reason why this mechanism should give a wider range of $\Delta G^{\ddagger}$ values than the butadiene rotation mechanism. Both mechanisms involve intramolecular rearrangements and should be affected by steric and electronic factors to approximately the same degree.

The second basis for ruling out the trigonal-twist mechanism was based on an error of reasoning. A nuclear Overhauser enhancement experiment performed on $HfPh(\eta^4\text{-}C_4H_6)[N(SiMe_2CH_2PMe_2)_2]$ showed that irradiation of the *o*-phenyl protons of the Hf−Ph group resulted in the enhancement of only one of the two Si−Me resonances seen at high temperatures.[28] Whereas Fryzuk's paper states that this observation is inconsistent with the trigonal-twist mechanism, this statement is incorrect: even in the *fac* configuration, one of the two silylmethyl groups on each arm of the amidophosphine ligand is closer to the Hf−Ph group than the other. The two Si−Me groups will therefore remain inequivalent (and will exhibit different NOEs) even if the *mer* to *fac* isomerization process is rapid; thus, the trigonal-twist mechanism is completely consistent with the results of the NOE experiment.

Since the butadiene rotation mechanism cannot account for the dynamic behavior of the $TiMe_2(\eta^4\text{-}C_4H_4R_2)$(dmpe) and the $M(\eta^4\text{-}C_4H_6)_2$(dmpe) complexes, whereas the trigonal-twist mechanism accounts for the behavior of these species as well as Fryzuk's complexes, we propose that the trigonal-twist (or a similar mechanism involving a five-coordinate intermediate) is the fluxional process in all of these compounds.

Acknowledgment. We thank the National Science Foundation (Grant CHE No. 89-17586) for support of this research. We thank Charlotte Stern and Teresa Prussak-Wiekowska of the University of Illinois X-ray Diffraction Laboratory for assistance with the X-ray crystal structure determination, and M.D.S. thanks the University of Illinois Department of Chemistry for a fellowship.

Supporting Information Available: Tables of atomic coordinates, calculated hydrogen positions, thermal parameters, and all bond distances and angles for $TiMe_2(\eta^4\text{-}C_4H_4Ph_2)$(dmpe), **2**, and $Ti(\eta^4\text{-}C_4H_6)_2$(dmpe), **4**, and figures of the observed and simulated butadiene ^1H NMR resonances for $TiMe_2(\eta^4\text{-}C_4H_6)$(dmpe), **1**, and $Ti(\eta^4\text{-}C_4H_6)_2$(dmpe), **4** (26 pages). Ordering information is given on any current masthead page.

OM9606552